RSC Advances

ROYAL SOCIETY OF CHEMISTRY

www.rsc.org/advances

Journal Name

RSCPublishing

ARTICLE

Synthesis of gold and palladium nanoshells by *in situ* generation of seeds on silica nanoparticle cores

Cite this: DOI: 10.1039/xoxxooooox

Elissa Grzincic,[a†] Ruishen Teh,[a†] Rachel Wallen,[a] Gabrielle McGuire,[a] Avinash Yella,[b] Ben Q. Li[b] and Krisanu Bandyopadhyay*[a]

Received ooth January 2012,
Accepted ooth January 2012

DOI: 10.1039/xoxxooooox

www.rsc.org/

This report describes the synthesis of silica–metal core–shell nanostructures by *in situ* generation of metal seeds on polyethyleneimine silane functionalized silica core surfaces eliminating the need for pre-synthesized metal seeds and a subsequent aging step, currently essential for synthesis of these materials. Specifically, gold nanoshells are generated on silica cores of two different sizes (~150 and ~40 nm diameter) following this *in situ* seed generation method. In addition, aqueous suspension of gold nanoshells with ~150 nm silica core and ~18 nm shell thickness shows characteristic photo-thermal property with ~16°C temperature change occurring from room temperature (25°C) within ~10 minutes when exposed to an 808 nm wavelength laser. This *in situ* seed-mediated synthesis is further extended to palladium nanoshells (on ~200 nm diameter silica core), and this paper reports for the first time the synthesis of palladium nanoshells from *in situ* generated palladium seeds on a silica core, unlike earlier reports of palladium nanoshell synthesis using solely gold nanoparticles as seeds to grow the final palladium shell. Different palladium shell thicknesses are generated by varying the concentration of seed-attached silica cores during the final synthesis step. For both gold and palladium nanoshell synthesis, ultraviolet–visible spectroscopy and transmission electron microscopy are used to follow the different steps of this synthesis process. The results demonstrate that this *in situ* seed generation method is effective for gold nanoshell synthesis with varying core sizes as well as being able to produce nanoshells with different metal overlays.

1. Introduction

Core–shell nanoparticles each with a dielectric silica core and a thin metal shell have attracted much attention due to their unique photo-physical properties and application possibilities ranging from catalysis to optical devices and medicine.[1, 2] Following the seminal work of Halas's group, [3] there have been an increased number of studies, in particular revolving around gold nanoshells, due to their characteristic optical and photo-thermal properties.[4, 5] It is well known now that optical properties of gold nanoshells can be tuned from the ultraviolet–visible (UV-Vis) to near-infrared (NIR) range by changing the ratio of core diameter to shell thickness.[3, 6] Due to their unique ability to absorb and disperse NIR radiation, gold nanoshells have already found application in biology and medicine for visual detection and therapeutic application towards cancer remediation,[2, 7] as an example. Fabrication of these types of nanostructures, capable of absorbing electromagnetic radiation in a narrow range of 700–900 nm, is particularly important for such therapeutic applications as tissues and cells are not affected by this range of radiation.[8, 9] Specifically, in photo-thermal therapeutic applications, it is possible to locally heat cancer tissues and destroy them by using appropriate electromagnetic radiation in combination with specific core–shell nanoparticles.[2] In addition to applications based on their optical properties, nanoshells are also finding use as photo-activated and photo-stabilized catalysts.[1] Towards this end, a palladium nanoshell is one of the predominant candidates due to the well-known catalytic properties of palladium nanoparticles which can be used as heterogeneous catalysts for diverse reactions including hydrogenation of olefins and dienes,[10, 11] hydration of acrylonitrile to acrylamide,[12] photo-generation of hydrogen from water,[13] and oxidation of alcohols.[14, 15] Very recently, catalytic activities of palladium nanoshells have been explored for the Suzuki–Miyaura cross-coupling reaction between phenylboronic acid and iodobenzene.[16] The ability to tune the plasmon resonance of gold nanoshells from visible to NIR wavelengths which spans nearly the entire solar spectrum that reaches the earth's surface has also opened up the possibility of using these systems in solar thermal absorption.[17-19] Currently, seed-mediated synthesis is the most commonly and widely used method to generate different nanoshell structures.[1] In this multistep synthesis process, 3-aminopropyltrimethoxysilane-modified silica nanoparticles are used as core, followed by attachment of gold nanoparticle seeds through electrostatic interaction between protonated amine functional groups on the silica surface with negatively charged gold nanoparticles prepared separately in solution. In the final step, a continuous gold shell is formed through growth of surface-attached gold nanoparticle

seeds and coalescence of the gold islands into a continuous overlayer.[20-22] This step is achieved by reduction of $Au(OH)_4^-$ generated in a reaction between $HAuCl_4$ and K_2CO_3 in solution in the presence of formaldehyde as reducing agent. For palladium nanoshell generation, only the final growth step is different from the gold nanoshell synthesis, where dilute acidic $PdCl_2$ solution is used in combination with L-ascorbic acid as reducing agent.[16, 23, 24] It is important to note that palladium nanoshells are also generated using surface-bound gold nanoparticles as seeds, and any attempt to use palladium seeds to grow palladium nanoshells has so far been unsuccessful.[16] As mentioned earlier, synthesis of metal nanoshells, specifically gold and palladium, involves pre-synthesized precursor gold nanoparticle seeds and subsequent aging of these seeds for at least 3 days to even 2 weeks.[1] In current methods, tetrakis(hydroxymethyl)phosphonium chloride is the most commonly used reducing agent to generate negatively charged 1–3 nm diameter gold nanoparticle seeds.[25] It is known that the aging time of these gold seeds is a key parameter to achieve the required surface coverage of seeds on silica core which in turn is critical to get a final uniform metal shell. During the aging process, size, pH and surface charge of gold nanoparticles change due to changes in their surface chemistry. Several days of aging is required before these nanoparticles can be stabilized to their final size (2–3 nm in diameter) so as to be subsequently effective as surface-attached seeds on the silica core.[1] An earlier report shows that gold nanoparticles aged for one week can generate a uniformly covered silica core as opposed to non-uniform distribution for those aged for a day.[1] Although the current method of using pre-synthesized gold seeds for nanoshell generation is effective, it heavily depends on the quality of the gold nanoparticle seeds prepared in solution and also requires extended synthesis time. Considering the application potential of these materials, it is critical to develop a general preparative route to synthesize different metal nanoshells without the need of separately pre-synthesized nanoparticle seeds.

Herein, we report the synthesis of gold and palladium nanoshells from *in situ* generated gold and palladium seeds on silica nanoparticle cores. The *in situ* generated seed metal nanoshell synthesis steps are shown in Scheme 1. Silica cores are synthesized in the first step through the well-known Stöber method,[26] followed by surface modification of these silica cores with trimethoxysilylpropyl-modified polyethyleneimine (TSPEI). The imine nitrogens present on the molecular backbone of TSPEI provide positively charged surface functional groups which are capable of capturing negatively charged metal precursor ions (like $[AuCl_4]^-$ or $[PdCl_4]^{2-}$) from solution through electrostatic interaction. Appropriate metal nanoparticle seeds are generated by reducing the surface-bound complex metal ions which are subsequently used as nucleation sites to grow different metal overlayers in the presence of a growth solution. An earlier approach reported on *in situ* generation of seeds on silica cores through the deposition-precipitation (DP) method[27-29] that required elevated temperature (60-80°C) and careful adjustment of pH (pH range 6-10) to be successful. In addition, the DP method is limited to gold nanoshell generation. In another report, poly(ethylenimine) (PEI) is used as linker and reductant for *in situ* generation of Ag and Au nanoparticles on polystyrene, silica and ZnO cores. This method requires specific pH adjustment during PEI modification step and elevated temperature (100°C) to generate metal nanoparticles. In addition, subsequent formation of only Ag-SiO_2 composites with different surface coverage of Ag on silica cores is reported.[30] An effort to grow a gold shell using the gold salt chloro(tetrahydrothiphene)gold(I) attached to an amine-functionalized silica core after displacement of tetrahydrothiphene has also been unsuccessful.[31] It is also to be noted that in all previous reports of any palladium or Au–Pd bimetallic nanoshell synthesis, only preformed gold seeds were used for final palladium shell formation,[16, 23, 24, 32] and use of

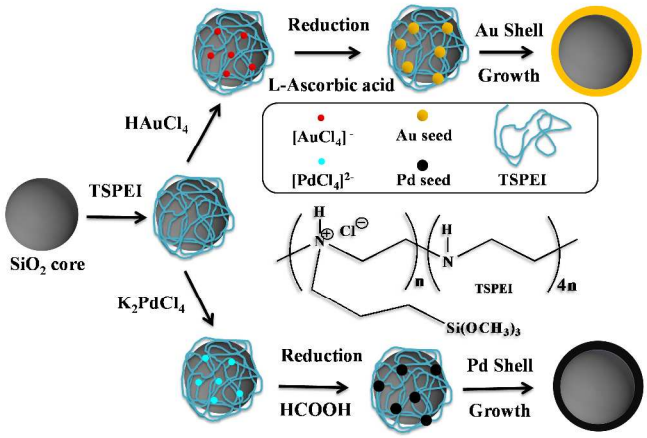

Scheme 1 Schematic of different steps involved in the synthesis of gold and palladium nanoshells by *in situ* generation of corresponding metal seeds on silica core surfaces.

palladium seeds was unsuccessful in generating the final palladium overlayer.[16] In light of the existing nanoshell synthesis procedure, our *in situ* seed generation procedure to synthesize gold and palladium nanoshells has a number of significant advantages over the current method. Most importantly, it eliminates any requirement of pre-synthesized seeds and subsequent extended aging (at least 3 days) step necessary before they can be attached to silica cores. In addition, our *in situ* seed-mediated nanoshell synthesis procedure is applicable for the generation of nanoshells with varying shell thickness and also for the synthesis of shells of various metals. This procedure provides a room temperature wet chemical approach without the need of stringent control of any experimental parameters like pH, temperature, etc. The present method provides a much faster synthesis route to generate gold and palladium nanoshells. We envision that with judicious selection of surface functionalization, it is possible to generate other metal nanoshells like Ag, Cu or Ni which also show a number of potential application possibilities.[1]

2. Materials and methods

2.1. Chemicals

For all experiments, water was purified through a Millipore system, the water having a resistivity of 18 MΩ cm. Tetraethyl orthosilicate (TEOS, 99.999%), gold(III) chloride trihydrate

($HAuCl_4.3H_2O$, 99.9+%), potassium tetrachloropalladate(II) (K_2PdCl_4, 99.99%), potassium carbonate (99.0%), formaldehyde (37 wt% in water), L-ascorbic acid, formic acid (88%), 200 proof (absolute) ethanol, NH_4OH (29% ammonia in water) and 2-propanol (99.5%) were obtained from Sigma-Aldrich (St Louis, MO) and were used as received. Concentrated sulfuric acid, 70% nitric acid and concentrated hydrochloric acid came from Fisher Scientific (Pittsburgh, PA) and TSPEI as a 50% solution in isopropanol was purchased from Gelest Inc. (Morrisville, PA) and used without further purification. Extra-dry compressed nitrogen gas was purchased from Metro Welding (Detroit, MI).

2.2. Characterization

Different nanoshells and silica cores were characterized using transmission electron microscopy (TEM) and UV-Vis spectroscopy. In addition, laser heating profile experiments for silica cores and gold nanoshells were carried out by passing a laser beam with a wavelength of 808 nm through a quartz cuvette with 3 mL of nanoshell solution and measuring the change in temperature with a temperature probe and an Agilent HP 34420A nano-voltmeter. The setup consisted of a laser (3 W) with beam diameter ~2 mm. The laser was incident on the cuvette containing the gold nanoshells, while at the open end of the cuvette a thermocouple was placed to measure the temperature change. The thermocouple was connected to a nano-voltmeter where the temperature output from the thermocouple was recorded. The distance from the tip of the thermocouple to the outer edge of the beam was 15 mm. TEM images were generated using a Hitachi HT7700 TEM, with an operating voltage of 100 kV. TEM samples were prepared by deposition of nanoshells dispersed in ethanol onto 200 mesh copper-coated, carbon-stabilized lacey Formvar support film grids and dried at room temperature. UV-Vis-NIR spectra were acquired using an Ocean Optics USB4000 fiber optic spectrometer with a Mikropack DH-2000-Bal UV-Vis-NIR light source over a range from 300 to 900 nm using a quartz cell having a path length of 1 cm.

2.3. Synthesis of silica nanoparticle cores

Syntheses of silica nanoparticle cores were carried out by a modified Stöber method.[26] Specifically, 9 M NH_4OH solution was prepared using a stock solution of 29% NH_3 in H_2O. 75 mL of 200 proof ethanol was added to 25 mL of H_2O, followed by addition of 3.5 mL of 9 M NH_4OH. After stirring the solution for 5 minutes, a 3 mL aliquot of TEOS was added quickly. The solution was stirred for 8 hours as the colorless solution changed to milky white within 20 minutes. Finally, three washing cycles were done using 99% ethanol and centrifuging at 4000 revolutions per minute (rpm) for 25 minutes at room temperature to ensure removal of excess unreacted chemicals. These reactant concentrations produced spherical silica nanoparticle cores of diameter ~200 nm as characterized by TEM. The typical concentration of these solutions was calculated to be ~8.2×10^{11} silica nanoparticles/mL assuming that all of the TEOS reacted and the density of these silica nanoparticles was 2 g/cm^3.

For ~150 nm silica nanoparticles, 8 mL NH_4OH (9 M) was added to 100 mL 200 proof ethanol in an Erlenmeyer flask with stirring. To this solution, 4.4 mL TEOS was added dropwise, and the solution was left stirring for 8 hours. After generation of silica nanoparticles, similar washing cycles were followed as described above. The typical ~150 nm silica core concentration was ~1.2×10^{12} per mL.

Silica core nanoparticles (~41 nm) were formed by adding 0.8 mL of NH_4OH and 6 mL of deionized water to a mixture of 50 mL of 200 proof ethanol and 50 mL of 2-propanol in an Erlenmeyer flask with stirring. The solution was then transferred to an AtmosBag (flexible, inflatable polyethylene chamber with built-in gloves, Sigma-Aldrich) filled with extra-dry nitrogen gas followed by drop-wise addition of 4.4 mL TEOS by a syringe pump from New Era Pump System Inc. (Farmingdale, NY). TEOS was used without prior purging of nitrogen gas. Stirring of the solution was continued for an additional 8 hours. At this stage, it was very difficult to spin down the ~ 40 nm diameter silica nanoparticle cores as a compact pellet even after applying a much higher centrifuge speed (> 4000 rpm). Therefore, we proceeded with the as prepared ~40 nm silica nanoparticles core solution to the functionalization step with TSPEI. Silica core concentration in this case was ~1.5×10^{14} per mL. It was noted during the synthesis of silica nanoparticle cores of different diameter that the solution appeared close to colorless for smaller silica cores compared to opaque and milky white for larger cores. Depending on the size range of silica nanoparticle cores, a 30- to 60-minute induction period was required before the solution changed color indicating the nucleation of silica cores from TEOS monomer. In addition, redispersing pellets of larger cores after centrifugation was more difficult compared to silica cores with smaller diameter.

2.4. Amine-functionalized silica core synthesis

In a typical experiment, 5 mL of silica core nanoparticles dispersed in absolute ethanol was diluted to 90 mL followed by addition of 10 mL of TSPEI (50% in isopropanol) solution to form a 5% by volume TSPEI solution. The reaction was carried out in a 250 mL round-bottom flask and was refluxed for one hour at 80°C, followed by an additional one hour of stirring without any heat. At this stage, the solution changed color from milky white to translucent white. Five washes were performed using 95% ethanol to remove excess TSPEI through centrifugation. The TSPEI-modified silica nanoparticles were centrifuged in a 5804 Refrigerated Centrifuge (Eppendorf) at 3500 rpm for 30 minutes and redispersed in 20 mL 95% ethanol by sonication for 5 minutes. Centrifugation, sonication and washing were repeated 5 times, and the functionalized silica nanoparticle cores were then left as a pellet overnight.

2.5. Adsorption of $[AuCl_4]^-$ or $[PdCl_4]^{2-}$ ions to TSPEI-functionalized silica cores

To adsorb $[AuCl_4]^-$ ions from solution, TSPEI-modified silica nanoparticle pellet was redispersed in 30 mL freshly prepared 1×10^{-2} M aqueous $HAuCl_4$ solution and agitated for approximately 5 minutes. The centrifuge tube containing the solution was wrapped in aluminum foil and allowed to stand at room temperature for 8 hours. The solution was then centrifuged at 3500 rpm for 30 minutes and redispersed in 10 mL deionized water. The solution was then again sonicated for 5 minutes. Centrifugation, sonication and washing were repeated 5 times, and the nanoparticles were then left overnight as a pellet. In this step $HAuCl_4$ solution was clear and bright yellow before mixing with silica cores after which it gradually turned brown upon mixing. Actually the cores became brown as evident from the brown-colored pellet with clear yellow supernatant solution.

For $[PdCl_4]^{2-}$ ion adsorption, a 30 mL solution of 1×10^{-2} M aqueous K_2PdCl_4 was made and the pellet of amine-functionalized silica cores was redispersed into the solution.

Subsequently, the solution was vortexed and stirred for 5 minutes with a color change from white to deep yellowish brown. This solution was then kept in the dark at room temperature for 8 hours before applying 5 washing cycles using water.

2.6. *In situ* generation of gold or palladium seeds on functionalized silica cores

The silica/TSPEI/$[AuCl_4]^-$ pellet was redispersed in a 2% (w/v) aqueous L-ascorbic acid solution with immediate change in color to dark blue or dark purple. The resulting solution was agitated for approximately 5 minutes, and allowed to stand in the dark at room temperature for 8 hours. The solution was then centrifuged at 3500 rpm for 30 minutes to get a dark blue/purple pellet which was subsequently redispersed in 30 mL deionized water. To generate palladium seeds from surface-attached $[PdCl_4]^{2-}$ ions, formic acid was used as reducing agent. A 2% (w/v) aqueous formic acid solution was made by dissolving 681.8 µL of formic acid (88% formic acid in H_2O) in 30 mL of water. After stirring for a few minutes, the solution was added to the silica/TSPEI/$[PdCl_4]^{2-}$ pellet with a color change from yellow to a dark brown. The solution was kept in the dark for 8 hours and washed 5 times using water before continuing to the next step.

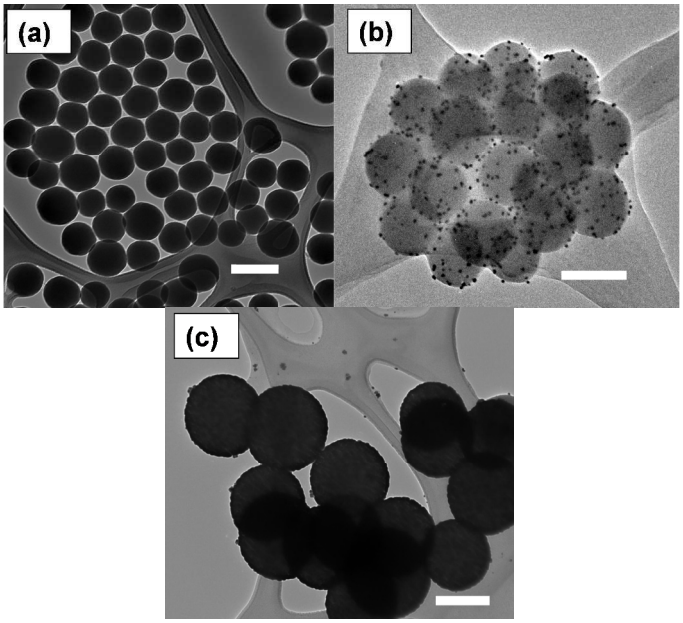

Fig. 1 TEM images: (a) ~150 nm diameter silica core nanoparticles; (b) silica core with attached ~13 nm gold nanoparticle seeds generated by *in situ* reduction of surface-bound $[AuCl_4]^-$ ions with 2% (w/v) aqueous L-ascorbic acid; (c) gold nanoshells, ~18 nm thick, on silica core. All scale bars are 200 nm.

2.7. Synthesis of gold and palladium nanoshells

A 25 mM aqueous $HAuCl_4$ solution (10.0 mL) was stored in the dark at 4°C for one day before it was used in the growth solution. The growth solution for gold nanoshell synthesis was prepared by adding 12.5 mg K_2CO_3 to 50 mL deionized water and stirring for 5 minutes followed by addition of 0.75 mL aged $HAuCl_4$ solution with stirring until it changed color from light yellow to clear, indicating the formation of gold hydroxide. The growth solution was then aged in the dark for one day at room temperature before further use. To grow a gold shell on each silica/TSPEI/$[AuCl_4]^-$ nanoparticle, 100 µL of the silica/TSPEI/Au nanoparticle solution was added to 9 mL of colorless growth solution with vigorous stirring. The stirring was continued for approximately 5 minutes before 80 µL of formaldehyde was added to the solution. At this point, the solution changed from colorless to blue over 1–2 min, indicating gold nanoshell formation. Stirring of the resulting solution was continued for an additional hour before the solution was centrifuged at 3500 rpm for 30 minutes and the resulting pellet was redispersed in deionized water until required for further use.

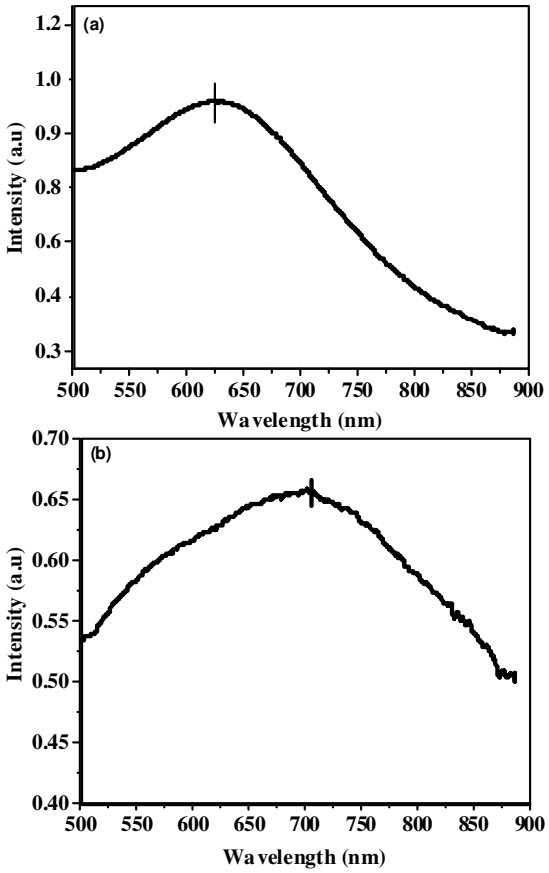

Fig. 2 UV-Vis spectra: (a) aqueous solution of ~150 nm diameter silica core with surface-bound *in situ* generated ~13 nm gold nanoparticle seeds; (b) aqueous dispersion of gold nanoshells grown from *in situ* generated gold seeds on silica core. Hash marks indicate the peaks of the spectra.

Similar to gold nanoshell synthesis, 25 mM K_2PdCl_4 solution was made by dissolving 0.0489 g K_2PdCl_4 in 6 mL water for palladium nanoshell generation. This solution was stored in the dark at 4°C for one day before use. A growth solution was prepared by dissolving 12.5 mg K_2CO_3 in 50 mL water along with 0.75 mL of 25 mM K_2PdCl_4 solution. At this stage the solution color changed from colorless to deep yellow. The growth solution was stored in the dark for one day at room temperature before further use. For subsequent palladium seed-mediated shell growth, 1.7612 g of ascorbic acid was dissolved in 10 mL of water (1 M) which was used as mild reducing agent. For palladium nanoshell growth, 100 µL of the silica/TSPEI/$[PdCl_4]^{2-}$ nanoparticles was dispersed in 9 mL of

the growth solution and the mixture was stirred for 5 minutes to form a yellow solution. Finally, 1.2 mL of the ascorbic acid solution was added to the above solution to complete the palladium shell growth. The color of the resulting solution changed from yellow to black within 20 minutes. The solution was stirred continuously for a total of 1.5 hours and was allowed to stand overnight. Over the course of this time, palladium nanoshells settled at the bottom of the tube as black precipitate leaving the supernatant colorless. The palladium nanoshells were then centrifuged and washed with water 5 times without any sonication. Finally the pellet was redispersed in water and stored in a refrigerator for future characterization.

3. Results and discussion

In this study, silica cores of three different sizes are synthesized by a modified Stöber procedure.[26] First, ~150 nm silica cores are generated to evaluate the feasibility of this new *in situ* generated seed method for the synthesis of gold nanoshells. Fig. 1(a) shows a TEM image of the dielectric silica cores with low polydispersity. These silica cores are then functionalized with amine-terminated surface silanizing agent TSPEI to attach $[AuCl_4]^-$ (tetrachloroaurate) ions from solution followed by *in situ* generation of Au nanoparticle seeds through ascorbic acid reduction. Fig. 1(b) shows a representative TEM image of silica cores decorated with Au seeds. Analysis of a number of such TEM images suggests the size of these Au seeds to be 13.4 ± 3.3 nm and they are distributed uniformly throughout the silica core surface. It is to be noted that the surface-attached seeds generated in this case are larger in size compared to pre-synthesized seeds used in regular nanoshell synthesis procedures.[3, 31, 33] Finally, these seeds are used as nucleation sites to generate Au shells (Fig. 1(c)) using a growth solution with formaldehyde as reducing agent. As expected from the previous studies of Au nanoshell generation using formaldehyde, the TEM image in Fig. 1(c) confirms the formation of complete Au shells with distinctly smooth surface morphologies. In addition, comparison of the TEM image of silica cores (Fig. 1(a)) with Fig. 1(c) suggests a gold shell thickness of ~18 nm.

We also followed the *in situ* Au seed generation on silica cores and subsequent nanoshell formation steps by tracking the unique optical properties through UV-Vis spectroscopy. Specifically, Fig. 2(a) shows an absorption band centered around 624.8 nm which is due to the collective surface plasmon of gold nanoparticle seeds, generated on silica core as shown by the TEM image in Fig. 1(b). It is known that absorption maxima for ~13 nm diameter Au nanoparticle in aqueous solution appear at ~522 nm.[34] This significant red-shift of surface plasmon band for immobilized Au seeds on silica core is due to the interaction of the closely spaced Au nanoparticles leading to a breakdown of the dipole approximation and points towards an aggregated nanoparticle structure.[32, 35] Similar observations have also been reported during the generation of two-dimensional assemblies of Au nanoparticles on functionalized surfaces.[34, 36] Upon Au nanoshell formation, the UV-Vis absorption maximum due to Au surface plasmon red-shifts to 702 nm as shown in Fig. 2(b), indicating the formation of a complete gold shell.[3, 31] Existing literature on gold nanoshell synthesis and prediction from the Mie theory suggest that the position of absorption maxima of gold nanoshell surface plasmon resonance is strongly dependent on both the shell thickness and the size of the dielectric silica core. It is further noted that during nanoshell growth, the UV-Vis maximum steadily shifts to longer wavelength as the shell grows and a thin shell shows absorption at a longer wavelength. Once a complete shell is formed, further increase in shell thickness shifts the nanoshell absorption maximum to shorter wavelength.[3] Considering the thick Au shell generated in this case, UV-Vis response of these nanoshells correlates well with the position of the absorption maximum reported in the literature and its narrow shift of ~77 nm in going from *in situ* generated Au seeds to complete shell formation.[3, 6]

One of the most prominent applications of these gold-coated silica nanoshells has emerged in the area of photo-thermal therapy.[5] By varying the size of the silica core and the thickness of the shell, it is possible to tune the plasmonic response of gold nanoshells to generate mild-temperature hyperthermia (<45°C) upon illumination with NIR light.[8] The combined use of NIR radiation and gold nanoshell absorber in photo-thermal therapy provides a critical advantage in protecting healthy tissue from thermal damage. It is possible to generate nanostructures capable of absorbing electromagnetic radiation and effectively

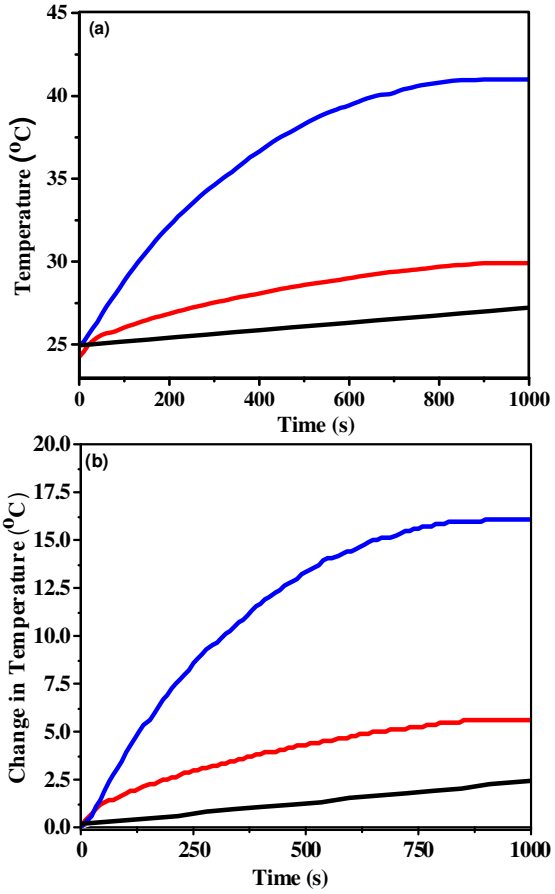

Fig. 3 (a) Comparative time-dependent temperature profile of water (black), aqueous suspension of ~150 nm silica nanoparticle cores (red) and aqueous dispersion of gold nanoshells with shell thickness ~18 nm (blue) under illumination of an 808 nm laser. (b) Data in (a) plotted as a function of change in temperature (ΔT) against time. For photothermal experiment, 3 mL of aqueous dispersion of Au nanoshell (1.7 mg mL^{-1} Au concentration) is exposed to 808 nm laser.

converting it to heat in a narrow wavelength range of 700–900 nm in possible therapeutic applications for various internal diseases, since water in tissues, hemoglobin in blood and melamine in skin do not absorb or are affected by this radiation. In order to assess the heating response of the gold nanoshells generated by the present *in situ* method, we measured the heating profile of an aqueous dispersion (1.7 mg mL^{-1} Au concentration) of these gold nanoshells with time under illumination of an 808 nm laser. Nanoshells concentration is calculated using density of Au as 19.32 g cm^{-3} and using specific core and shell dimensions from the analysis of TEM images. Fig. 3(a) shows a typical heating response of gold nanoshells in comparison with water and also an aqueous dispersion of bare silica cores. It is evident that the temperature of the gold nanoshells gradually increases up to ~41°C from room temperature (25°C) before a temperature plateau is observed beyond 10 minutes of heating time. Both water, which is used as a base liquid for dispersing gold nanoshells, and 150 nm silica cores in water only show very minimal change in temperature in comparison with the gold nanoshells. These temperature changes are more apparent when the same data in Fig. 3(a) are plotted as a change in temperature (ΔT) with time,

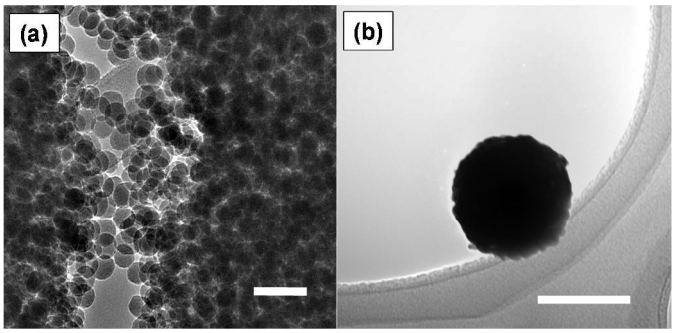

Fig. 4 TEM images of (a) ~40 nm diameter silica core nanoparticles and (b) gold nanoshell of ~28 nm in thickness on 40 nm silica core. Scale bars are 100 nm.

as presented in Fig. 3(b). A significant temperature raise of ~16°C is observed for aqueous suspension of gold nanoshells compared to 1.4°C and ~6.0°C for pure water and aqueous suspension of silica cores respectively. It is important to note that the maximum temperature change is achieved within ~10 minutes exposure of the gold nanoshell suspension to laser illumination.

It is true that additional factors need to be considered other than only size to improve nanoshell biodistribution for any photo-thermal therapeutic application.[2] However, nanoshell size is indeed a critical factor to achieve that goal.[37] Keeping that in mind, we have explored our current *in situ* seed generation method of gold nanoshell synthesis for relatively small (less than 100 nm diameter) nanoshells. It is known that synthesis of gold nanoshell with less than 100 nm diameter is challenging due to their tendency towards aggregation arising from the size dependent electrostatic double-layer potential. Silica cores of ~40 nm diameter have been synthesized for this purpose using 1:1 ratio of ethanol and 2-propanol instead of pure ethanol as solvent for the regular Stöber method.[26] It is known that solvent dielectric constant is an important factor in controlling the size of the silica core.[1] In our case, by changing the ratio of ethanol to 2-propanol we are able to generate silica cores with varying diameters smaller than 100 nm. A typical TEM image of ~40 nm (41.1 ± 6.0 nm) silica core nanoparticles is shown in Fig. 4(a). Subsequently, we modified these silica cores using TSPEI followed by absorption of $[AuCl_4]^-$ ions from solution and finally reducing the surface-bound $[AuCl_4]^-$ by ascorbic acid to generate Au seeds. Analysis of TEM images provides a seed size of 10.6 ± 3.3 nm (data not shown) which is comparable to the seeds generated on ~150 nm silica cores used in the previous case. These silica cores with surface-bound Au nanoparticles are then used for seed-mediated growth of Au

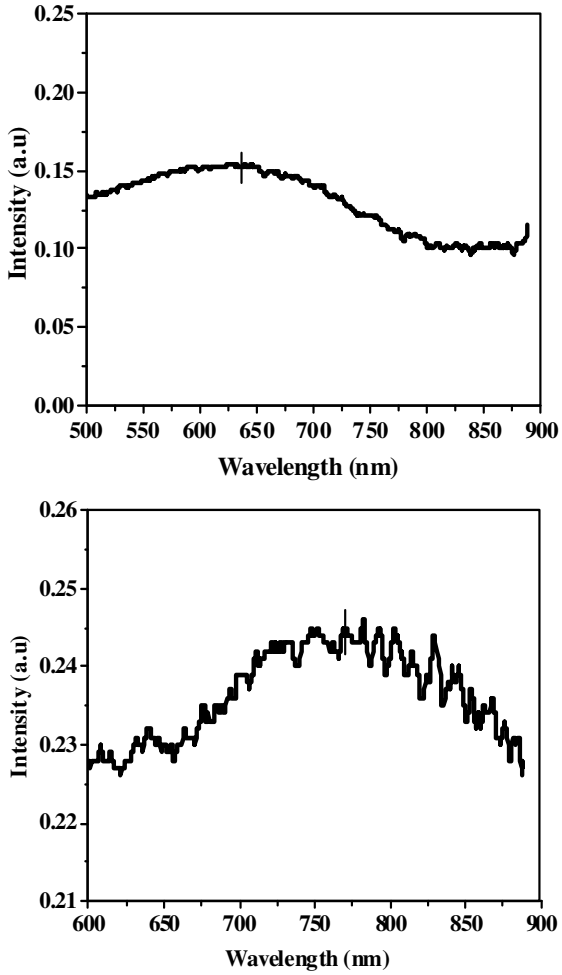

Fig. 5 UV-Vis spectra of (a) aqueous solution of *in situ* generated ~10 nm gold nanoparticle seeds attached to ~40 nm diameter silica core and (b) aqueous dispersion of gold nanoshells formed using *in situ* generated gold seeds on silica core. Hash marks indicate the peaks of the spectra.

shells following the same procedure applied before for the larger silica cores. A typical TEM image of a nanoshell in Fig. 4(b) when compared with bare silica cores in Fig. 4(a) indicates a shell thickness of ~28 nm.

We also followed the *in situ* gold seed generation and subsequent shell formation steps by tracking the surface plasmon features through UV-Vis spectroscopy. Fig. 5(a) shows a broad absorption maximum at ~630 nm for *in situ* generated gold nanoparticle seeds bound to 40 nm diameter silica core in solution. The absorption maximum due to surface plasmons for free ~10 nm Au nanoparticles in aqueous solution

is known to appear at ~520 nm.[38] Similar to gold nanoshell synthesis on 150 nm silica cores, significant red-shift of the surface plasmon band is also observed for immobilized gold seeds in this case.[35] It is observed in Fig. 5(b) that the surface plasmon band has further red-shifted with a broad absorption maximum at ~770 nm, indicating gold overlayer formation.

The absorption bands of smaller gold nanoparticles and gold

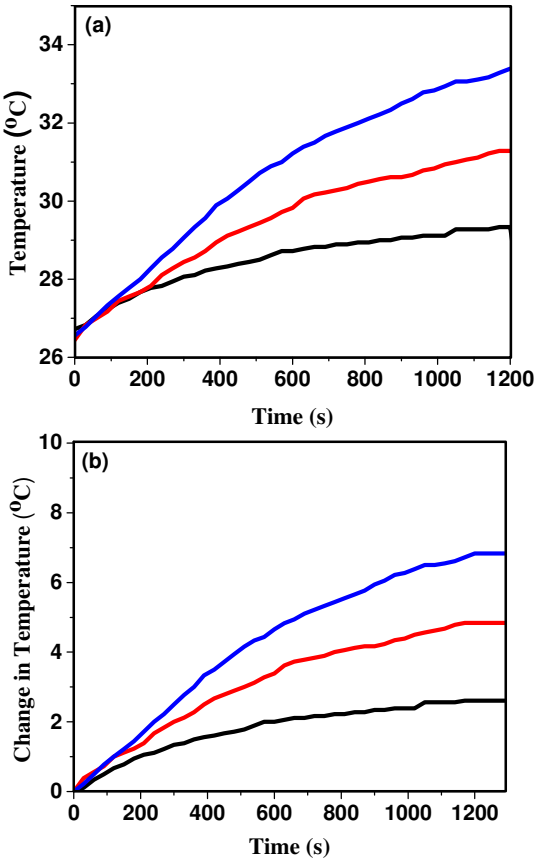

Fig. 6 (a) Comparative time-dependent temperature profile of water (black), aqueous suspension of ~40 nm silica nanoparticle cores (red) and aqueous dispersion of gold nanoshells with shell thickness ~28 nm (blue) under illumination of an 808 nm laser. (b) Data in (a) plotted as a function of change in temperature (ΔT) against time. For photothermal experiment, 3 mL of aqueous dispersion of Au nanoshell (0.42 mg mL^{-1} Au concentration) is exposed to 808 nm laser.

shells on smaller silica cores generally show absorption at a shorter wavelength than those of larger gold nanoparticles and gold shells on larger silica cores. If we compare UV-Vis response associated to gold nanoshell formation on ~150 nm and ~40 nm silica cores, it is evident that changes in wavelength of absorption bands going from *in situ* seed generation to gold nanoshell formation step fail to follow the expected trend mentioned above. Specifically, smaller gold seeds (~10 nm) on small silica cores (~40 nm) show absorption maximum at 630 nm (Fig. 5a), while gold seeds (~13 nm) on larger silica cores (~150 nm) exhibit absorption maximum ~ 624.8 nm (Fig. 2a). Similarly, the gold shells on smaller silica cores (~40 nm) possess absorption maximum at 770 nm (Fig. 5b), but the gold nanoshells on lager silica cores (~150 nm) exhibit absorption maximum at 702 nm (Fig. 2b). It is known that absorption maxima for ~10 nm and ~13 nm diameter Au nanoparticles in aqueous solution appear at ~520 nm and 522 nm respectively and these values are not much far apart. Red shift in absorption maxima is observed for both the Au seeds when generated onto ~40 nm and ~150 nm silica cores, with wavelength shift being more for surface-bound ~10 nm Au seeds compared to that of ~13 nm. In general, shift in absorption maxima is expected for supported Au nanoparticles due to surface plasmon coupling from individual Au nanoparticles located close to each other on silica nanoparticle core surface. The higher shift for smaller Au seeds may possibly be due to higher clustering of nanoparticle seeds on ~40 nm silica core surfaces as well as higher propensity of aggregation for smaller diameter silica cores. On the other hand, it is known from limited literature reports on smaller diameter Au nanoshell synthesis that high degree of aggregation occurs for smaller diameter nanoshells due to more diffuse charged double layer arising from their higher surface curvature compared to the larger diameter nanoshells.[37] Due to this significant aggregation, it is also difficult to measure shell thickness accurately by analyzing TEM images for smaller diameter nanoshells. Deviation from expected UV-Vis response for smaller diameter nanoshells may also be possible due to poly-dispersity and surface roughness in addition to aggregation.[37] Typical TEM image of an individual Au nanoshell on ~40 nm silica core in Fig. 4(b) and additional TEM images in Fig. S1 show a rough appearance of the nanoshell surface and suggests an aggregated structure of these nanoshells. It is known that rough edges can generate sites for localized electric field enhancements which can create plasmon oscillation modes at longer wavelengths than expected for Au nanoshells with smoother surfaces. Aggregations, on the other hand, can also create additional oscillation modes due to the complex geometry of the aggregate to affect the plasmon resonance.

Heating profile of aqueous dispersion of Au nanoshell on ~ 40 nm silica cores is also measured along with an aqueous dispersion of ~40 nm silica cores and pure water. Fig. 6 (a) and (b) represent typical temperature versus time and change in temperature (ΔT) versus time data respectively. It is certainly clear from these plots that temperature increases gradually with time for Au nanoshells on smaller diameter silica core. When compared with heating profile of larger diameter nanoshell in Fig. 3(a) and (b), it is evident that rate of temperature increase is much slower for smaller diameter nanoshell as well as the final temperature of the nanoshell suspension. It is known that initial temperature increase of the nanoshell suspension is indicative of the total energy absorption by the nanoshells and this type of temperature rise is due to transmittance of localized heat to the surrounding aqueous medium. Although it is known that larger Au nanoshells are relatively efficient energy absorber, the difference in steady state temperature increase between larger and smaller diameter nanoshells is primarily due to difference in gold concentration in the dispersion rather than initial size of the nanoshells.[39] If we focus on the temperature change associated with first 10 minutes exposure to the laser, ~16°C and ~4.6°C temperature changes are observed for larger (Fig. 3b) and smaller diameter (Fig. 6b) nanoshell suspension respectively. The increase in temperature at 10 minutes for these two aqueous suspensions with different diameter nanoshells scales roughly with the mass ratio of the Au

nanoshells. The larger diameter nanaoshells with Au concentration 1.7 mg mL^{-1} shows around 4 times increase in temperature compare (~16°C versus ~4.6°C) to smaller diameter nanoshell with 0.42 mg mL^{-1} Au concentration in the aqueous suspension.

In order to evaluate the applicability of this new *in situ* seed generation method to other metal nanoshell synthesis, we have extended the current procedure to palladium nanoshell synthesis. In our study, unlike the previously reported synthesis procedure of palladium nanoshells,[16, 23, 24] K_2PdCl_4 is used as palladium precursor instead of $PdCl_2$. Furthermore, all the previous reports of palladium metal nanoshell synthesis involve the use of gold seeds as nucleation sites to grow the final palladium overlayer, and any attempt to use palladium seeds

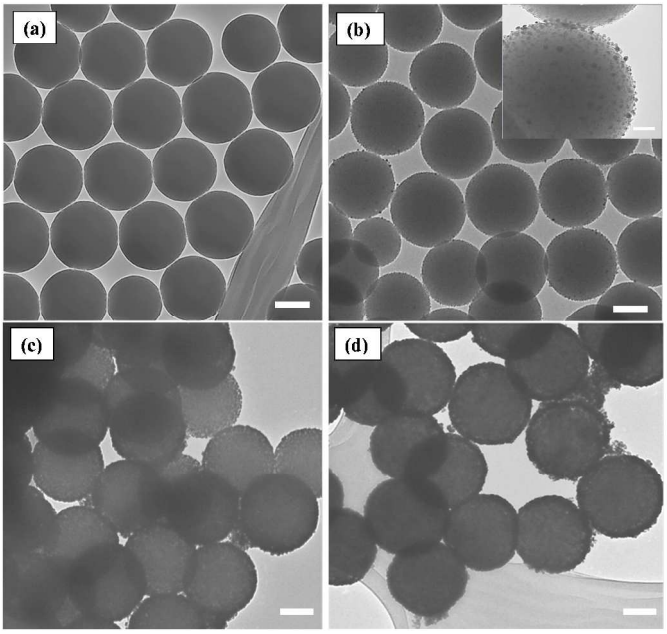

Fig. 7 TEM images: (a) ~200 nm diameter silica nanoparticle cores; (b) silica cores in (a) with attached palladium seeds of ~4 nm diameter; palladium nanoshells with thicknesses of (c) ~12 nm and (d) ~16 nm generated by using 100 µL and 50 µL of palladium seeds attached to silica cores in the final step of the palladium nanoshell synthesis process. Inset in (b) shows a magnified view of ~4 nm diameter *in situ* generated palladium seeds attached to TSPEI-modified silica core. These palladium seeds are generated by reduction of surface-bound $[PdCl_4]^{2-}$ ions with 2% (w/v) aqueous formic acid solution. All scale bars are 100 nm except for that of the inset in (b) which is 30 nm.

attached to silica cores to generate palladium shells has been unsuccessful. To the best of our knowledge, this is the first report of palladium nanoshell synthesis using palladium nanoparticles as seeds, generated *in situ* on functionalized silica cores to grow the final palladium shells. Fig. 7(a) shows a representative TEM image of ~200 nm (206 ± 18 nm) silica core nanoparticles that are used for palladium nanoshell synthesis. After functionalization of these silica cores with TSPEI and subsequent adsorption of $[PdCl_4]^{2-}$ ions, palladium seeds are generated *in situ* on the silica core surfaces which are evident from Fig. 7(b). The appearance of small dots on the silica core surface confirms the successful generation of palladium seeds, as shown in the inset of Fig. 7(b) which is a high-resolution TEM image showing a uniform distribution of palladium seeds of ~3 nm (3.6 ± 1.4 nm) diameter produced using formic acid as reducing agent. Fig. 7(c) and (d) show TEM images of palladium nanoshells with different Pd shell thicknesses obtained by varying the volume of palladium seed-tethered silica cores. Use of 100 µL (Fig. 7(c)) and 50 µL (Fig. 7(d)) silica cores with palladium seeds leads to ~12 nm and ~16 nm shell thicknesses respectively, as a lower concentration of palladium seeds attached to silica cores generates thicker shells.[24] Nanoshell surfaces are smooth in appearance, consistent with the finding that L-ascorbic acid is the preferred reducing agent for palladium shell synthesis.

We also followed the different steps towards palladium nanoshell formation using UV-Vis spectroscopy. Fig. 8 shows UV-Vis spectra of silica cores with attached $[PdCl_4]^{2-}$ ions, silica cores after *in situ* palladium seed formation and after palladium shell generation from palladium seeds attached to the silica cores, these shells having a thickness of ~12 nm. It is known that the UV-Vis spectrum of dilute aqueous solution of K_2PdCl_4 shows two strong ligand-to-metal charge transfer (LMCT) bands in the range 200–250 nm corresponding to the hydrolysis product $[PdCl_3OH]^-$.[40] The observed UV-Vis band at λ_{max} ~ 225 nm for silica cores after palladium ion adsorption in the form of $[PdCl_3OH]^-$ is due to LMCT band arising from interaction of the complex palladium anion with the secondary/tertiary nitrogen present in the backbone of the TSPEI layer on the silica cores.[41] This complexation is likely to occur through displacement of water from $[PdCl_3OH]^-$ leading to covalent reaction with the amine groups in TSPEI. Upon *in situ* reduction of these surface-bound palladium ions by formic acid, an absorption peak appears at λ_{max} ~ 226 nm which is characteristic of bare palladium nanoparticles of ~4 nm diameter,[42] correlating well with the palladium seed size (~3.4 nm diameter) generated in our case. Finally, this peak is completely absent after palladium shell formation with the appearance of a broad absorption at the specific wavelength range similar to that reported in the literature.[16, 23, 24]

We have also measured the heating profile of an aqueous dispersion of palladium nanoshells (0.53 mg mL^{-1} Pd concentration) with a shell thickness of ~12 nm (TEM image in Figure 6c). Fig. S2 (a) and (b), under supporting information, shows a comparative time-dependent heating profile of aqueous dispersion of Pd nanoshells, aqueous dispersion of ~200 nm diameter silica cores and pure water. No significant increase in temperature is observed for Pd nanoshell dispersion compared to water or aqueous silica cores dispersion. It is evident from the UV-Vis response of Pd nanoshells in Fig. 7(c) that no surface plasmon resonance band is present for Pd nanoshells in visible-NIR range, which is actually responsible for absorption of radiation and in turn for heat generation. Heat profile measurement thus conforms that no significant temperature changes (~4.2°C) is produced for Pd nanoshell dispersion under exposure to 808 laser.

In order to complete the study, we have generated gold nanoshells on ~200 nm diameter silica core nanoparticles. A detailed procedure describing different steps of synthesis is included under supporting information section. Figure S3 (a) and (b) shows the TEM images of gold nanoshells on ~200 nm silica cores. Gold nanoshell surface appears to be rough in nature and show that a thick shell has been formed. Comparison of TEM images of gold nanoshells (Fig. S3b) and of ~200 nm

silica core (Fig. 7a), reveals a shell thickness of ~23.6 nm as compared to ~18 nm gold shells on ~150 nm silica cores. UV-Vis spectrum in Fig. S3(c) shows a broad absorption maximum at ~678 nm which has blue shifted compared to ~18 nm thick gold nanoshells on ~ 150 nm silica cores (Fig. 2b) due to thicker nanoshells formation on ~200 nm silica cores.[3] However, these results demonstrate that our *in situ* seed-mediated nanoshell synthesis method is applicable to generate metal nanoshells onto silica cores of varying sizes.

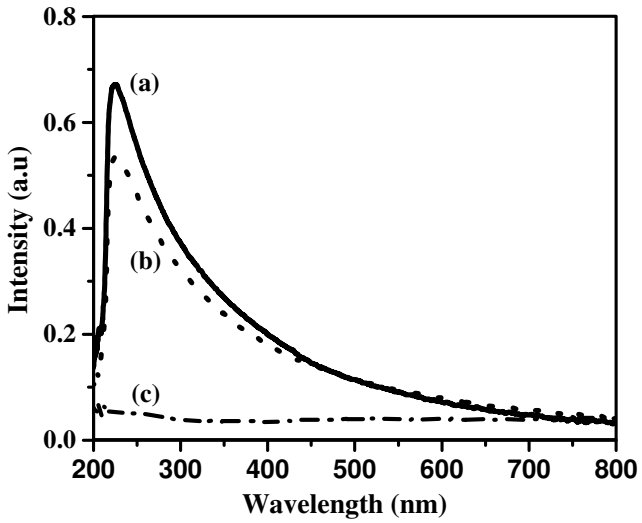

Fig. 8 UV-Vis spectra: (a) ~200 nm silica cores with attached $[PdCl_4]^{2-}$ ions; (b) after formation of ~4 nm diameter palladium seeds on the surface of silica cores by *in situ* reduction of $[PdCl_4]^{2-}$ ions; (c) after generation of ~12 nm thick palladium shells on ~200 nm silica cores.

4. Conclusions

The results presented have successfully demonstrated gold nanoshell synthesis using *in situ* generated gold seeds on silica core surfaces, eliminating the need for pre-synthesized gold seeds and also the subsequent aging process necessary in the currently used method to synthesize these materials. Silica cores with two different diameters (~150 nm and ~40 nm) are used to demonstrate the general applicability of this synthesis process involving *in situ* generated seeds. In addition, an aqueous suspension of Au nanoshells with 150 nm silica cores shows ~16°C temperature change within 10 minutes, while ~4.6°C increase in temperature is observed for nanoshells generated on ~40 nm silica cores, when exposed to an 808 nm wavelength laser, confirming their photo-thermal heating properties. This *in situ* seed-mediated nanoshell synthesis is further extended to generate palladium nanoshells on ~200 nm silica cores. Unlike all the previous reports of palladium nanoshell synthesis from gold seeds, the current method demonstrates, for the first time, the synthesis of palladium nanoshells from *in situ* generated palladium seeds on silica core surfaces. Moreover, palladium shells with varying thickness can also be prepared using different concentrations of seed-coated silica cores in the final shell growth step. UV-Vis spectroscopy is used to monitor the different steps involved in palladium nanoshell synthesis which shows the disappearance of the absorption peak for surface-bound palladium ions and *in situ* generated palladium nanoparticles to a broad featureless UV-Vis response upon palladium nanoshell formation. The presented *in situ* nanoshell synthesis method provides a simple yet versatile wet chemical approach to gold and palladium nanoshell synthesis at room temperature and can be extended to generate other metal nanoshells from their corresponding *in situ* generated seeds on silica core surfaces. Elimination of the need for pre-synthesized seeds and subsequent aging of seeds for at least 3 days will simplify the current method of synthesis of these materials to a great extent, enabling broader application possibilities of these core–shell materials.

Acknowledgements

We thank the American Chemical Society, Petroleum Research Fund and National Science Foundation (NSF) for financial support. Office of the Vice President for Research (OVPR), UM-Ann Arbor and the Office of Research and Sponsored Programs, UM-Dearborn are also gratefully acknowledged for additional funding. We also thank Rongheng Li for additional temperature profile measurements.

Notes and references

[a] *Department of Natural Sciences, University of Michigan – Dearborn, 4901 Evergreen Road, Dearborn, MI 48128, United States. Email: krisanu@umich.edu; Phone: +1- 313-593-5159; fax: +1- 313-593-4937*
[b] *Department of Mechanical Engineering, University of Michigan – Dearborn, 4901 Evergreen Road, Dearborn, MI 48128, United States*

†These authors contributed equally to this work.

Electronic Supplementary Information (ESI) available: Synthesis procedure of gold nanoshells on ~200 nm diameter silica core, additional TEM images of gold nanoshells on ~40 nm diameter silica core, comparative heating responses of aqueous dispersion of Palladium nanoshells on ~200 nm silica core, aqueous dispersion of ~200 nm silica core and water, and TEM and UV-Vis spectrum of gold nanoshells on ~200 nm diameter silica core. See DOI: 10.1039/b000000x/

1. B. J. Jankiewicz, D. Jamiola, J. Choma and M. Jaroniec, *Advances in Colloid and Interface Science*, 2012, **170**, 28-47.
2. L. C. Kennedy, L. R. Bickford, N. A. Lewinski, A. J. Coughlin, Y. Hu, E. S. Day, J. L. West and R. A. Drezek, *Small*, 2011, **7**, 169-183.
3. S. J. Oldenburg, R. D. Averitt, S. L. Westcott and N. J. Halas, *Chemical Physics Letters*, 1998, **288**, 243-247.
4. N. J. Halas, S. Lal, W.-S. Chang, S. Link and P. Nordlander, *Chemical Reviews*, 2011, **111**, 3913-3961.
5. S. Lal, S. E. Clare and N. J. Halas, *Accounts of Chemical Research*, 2008, **41**, 1842-1851.
6. L. Hirsch, A. Gobin, A. Lowery, F. Tam, R. Drezek, N. Halas and J. West, *Ann Biomed Eng*, 2006, **34**, 15-22.
7. R. Bardhan, S. Lal, A. Joshi and N. J. Halas, *Accounts of Chemical Research*, 2011, **44**, 936-946.
8. P. Diagaradjane, A. Shetty, J. C. Wang, A. M. Elliott, J. Schwartz, S. Shentu, H. C. Park, A. Deorukhkar, R. J. Stafford, S. H. Cho, J. W. Tunnell, J. D. Hazle and S. Krishnan, *Nano Letters*, 2008, **8**, 1492-1500.
9. R. J. S. Hirsch L.R, J. A. Bankson, S. R. Sershen, B. Rivera, R. E. Price, J. D. Hazle, N. J. Halas, and J. L. West, *Proc Natl Acad Sci U S A.* , 2003, **23**, 13549–13554.

10. Y. Niu, L. K. Yeung and R. M. Crooks, *Journal of the American Chemical Society*, 2001, **123**, 6840-6846.
11. W. Long, N. A. Brunelli, S. A. Didas, E. W. Ping and C. W. Jones, *ACS Catalysis*, 2013, **3**, 1700-1708.
12. N. Toshima and Y. Wang, *Advanced Materials*, 1994, **6**, 245-247.
13. A. J. Bard, *Science*, 1980, **207**, 139-144.
14. E. Rikkinen, A. Santasalo-Aarnio, S. Airaksinen, M. Borghei, V. Viitanen, J. Sainio, E. I. Kauppinen, T. Kallio and A. O. I. Krause, *The Journal of Physical Chemistry C*, 2011, **115**, 23067-23073.
15. C. Bianchini and P. K. Shen, *Chemical Reviews*, 2009, **109**, 4183-4206.
16. J.-H. Kim, J.-S. Park, H.-W. Chung, B. W. Boote and T. R. Lee, *RSC Advances*, 2012, **2**, 3968-3977.
17. N. Harris, M. J. Ford and M. B. Cortie, *The Journal of Physical Chemistry B*, 2006, **110**, 10701-10707.
18. W. Lv, P. E. Phelan, R. Swaminathan, T. P. Otanicar and R. A. Taylor, *Journal of Solar Energy Engineering*, 2012, **135**, 021004-021004.
19. B. J. Lee, K. Park, L. Xu and T. Walsh, *Journal of Solar Energy Engineering*, 2012, **134**, 021009-021009.
20. T. C. Preston and R. Signorell, *ACS Nano*, 2009, **3**, 3696-3706.
21. C. Sauerbeck, M. Haderlein, B. Schürer, B. Braunschweig, W. Peukert and R. N. Klupp Taylor, *ACS Nano*, 2014.
22. J. Polte, M. Herder, R. Erler, S. Rolf, A. Fischer, C. Wurth, A. F. Thunemann, R. Kraehnert and F. Emmerling, *Nanoscale*, 2010, **2**, 2463-2469.
23. J.-H. Kim, W. W. Bryan, H.-W. Chung, C. Y. Park, A. J. Jacobson and T. R. Lee, *ACS Applied Materials & Interfaces*, 2009, **1**, 1063-1069.
24. J.-H. Kim, H.-W. Chung and T. R. Lee, *Chemistry of Materials*, 2006, **18**, 4115-4120.
25. D. G. Duff, A. Baiker and P. P. Edwards, *Langmuir*, 1993, **9**, 2301-2309.
26. W. Stöber, A. Fink and E. Bohn, *Journal of Colloid and Interface Science*, 1968, **26**, 62-69.
27. N. Phonthammachai, J. C. Y. Kah, G. Jun, C. J. R. Sheppard, M. C. Olivo, S. G. Mhaisalkar and T. J. White, *Langmuir*, 2008, **24**, 5109-5112.
28. N. Phonthammachai and T. J. White, *Langmuir*, 2007, **23**, 11421-11424.
29. J. Y. Kah, N. Phonthammachai, R. Y. Wan, J. Song, T. White, S. Mhaisalkar, I. Ahmadb, C. Shepparda and M. Olivoc, *Gold Bull*, 2008, **41**, 23-36.
30. C. Tian, B. Mao, E. Wang, Z. Kang, Y. Song, C. Wang and S. Li, *The Journal of Physical Chemistry C*, 2007, **111**, 3651-3657.
31. T. Pham, J. B. Jackson, N. J. Halas and T. R. Lee, *Langmuir*, 2002, **18**, 4915-4920.
32. J.-H. Kim, W. W. Bryan and T. Randall Lee, *Langmuir*, 2008, **24**, 11147-11152.
33. B. E. Brinson, J. B. Lassiter, C. S. Levin, R. Bardhan, N. Mirin and N. J. Halas, *Langmuir*, 2008, **24**, 14166-14171.
34. C. J. Addison and A. G. Brolo, *Langmuir*, 2006, **22**, 8696-8702.
35. T. Okamoto and I. Yamaguchi, *The Journal of Physical Chemistry B*, 2003, **107**, 10321-10324.
36. A. F. Scarpettini and A. V. Bragas, *Langmuir*, 2010, **26**, 15948-15953.
37. M. R. Rasch, K. V. Sokolov and B. A. Korgel, *Langmuir*, 2009, **25**, 11777-11785.
38. J. H. Yoon, J. Lim and S. Yoon, *ACS Nano*, 2012, **6**, 7199-7208.
39. B. G. Prevo, S. A. Esakoff, A. Mikhailovsky and J. A. Zasadzinski, *Small*, 2008, **4**, 1183-1195.
40. L. I. Elding and L. F. Olsson, *The Journal of Physical Chemistry*, 1978, **82**, 69-74.
41. R. W. J. Scott, H. Ye, R. R. Henriquez and R. M. Crooks, *Chemistry of Materials*, 2003, **15**, 3873-3878.
42. A. Henglein, *The Journal of Physical Chemistry B*, 2000, **104**, 6683-6685.

Graphical Abstract

Synthesis of gold and palladium nanoshells by *in situ* generation of seeds on silica nanoparticle cores

Elissa Grzincic,[a†] Ruishen Teh,[a†] Rachel Wallen,[a] Gabrielle McGuire,[a] Avinash Yella,[b] Ben Q. Li[b] and Krisanu Bandyopadhyay*[a]

Gold and palladium nanoshells are formed on polyethyleneimine silane functionalized silica nanoparticle cores using *in situ* generated metal nanoparticle seeds.